



realizing the fractional order COs, are realized and their frequency responses are studied. This is being done to ensure whether the designed pseudo-capacitances have fractional behavior or not in the desired frequency and phase spectrum. It has been observed that the variation of fractional order ( $\alpha$ ) from 0.4 to 0.81 has resulted in a slight reduction of oscillation frequency from 1.68GHz ( $\alpha=0.4$ ) to 1.351GHz ( $\alpha=0.81$ ) keeping the pseudo-capacitance same at 0.3nF in MOS based topology. Further, CNTFET based integer order as well as fractional order COs have been designed to address the power consumption and the complexity issues of the fractional order COs. The CNTFET based fractional order CO retains the advantages of fractional order domain as well as power efficiency of CNTFETs. Furthermore, it has been observed that integrating fractional order capacitor (FOC) with the CNTFET CO results in much larger constant phase zone (CPZ), an important performance measuring parameter. A rigorous comparative analysis of the four COs designed in this work has been performed.

*Index Terms* : CNTFET, Fractional circuit, Oscillators, SPICE.

## INTRODUCTION

Oscillator circuits produce continuous and periodic sinusoidal waveforms of a particular frequency and work on the concept of positive feedback. The active elements like transistors, operational amplifiers, MOSFET etc. are used to provide the loop gain, however, the passive networks (including the tank circuit) yields positive feedback. Whenever the oscillator is excited by a dc source it responds by a steady state signal. The designing of oscillators is classified into families based upon the kind and number of memory elements in use [1-2]. The Colpitts oscillator (CO) family is one wherein the tank circuit has two capacitances and one inductor coil. It is employed for high frequency applications and is a preferred topology since it is simple and devoid of mutual inductance effects present between two inductors as in the case of Hartley oscillator [3-4]. Oscillators are mostly realized by integer order elements; however, recently researchers have shown a lot of interest in fractional order elements, like fractional order inductors and capacitors, due to various advantages of fractional order elements (FOE). Fractional order circuits have been found to be more accurate in reproducing the behavior of physical processes than the conventional integer order systems. Modeling examples have been found in rheology, mechanics, chemistry, physics, bioengineering, robotics and many scientific fields [5-8]. Fractance devices provide an additional degree of control over phase and frequency response due to the presence of fractional order,  $\alpha$ . Fractional order,  $\alpha$  gives an extra freedom due to which higher order systems can be represented using fewer coefficients. The fractional order capacitors (FOC) and fractional order inductors (FOI) are very important elements for fractional circuitry and are known to behave like constant phase elements (CPE). Over wide range of frequency the phase characteristics of systems designed using fractional elements is known to be constant, thus generating constant phase zones (CPZ). Mathematically, for an ideal resistor, capacitor and inductor,  $\alpha$  is '0', '1' and '-1' respectively. For a fractional order element,  $\alpha$  ranges from -1 to 1 and the magnitude of impedance varies with frequency according to  $\alpha$ . However, the realization of fractional elements using passive RC ladder circuitry results in increased circuit complexity, more power consumption and noise compared to the conventional integer order counterparts. Therefore, there is an immediate need to address the issues of complexity and power consumption in fractional order circuitry to retain its advantages [9-11,14-18]. The use of conventional complementary metal oxide semiconductor (CMOS) technology to realize FOC is a good choice, as it is well known for low power consumption, large noise margin (NM), large packing density etc. However, CMOS technology has its own limitations, particularly when scaled below 22 nm technology node. The MOS devices face severe short channel effects, gate oxide tunneling, increase in leakage, increase in sensitivity to process variations in integrated circuit manufacturing and increased fabrication cost [12-13]. Therefore, the need of the hour is to have new devices which can replace the existing silicon MOSFET, with clear-cut advantages and enabling efficiently new low cost applications. Carbon nanotube field effect transistor (CNTFET) is considered as a future device with extra ordinary properties due to the presence of CNTs in its channel. A CNTFET has large mobility, large transconductance ( $g_m$ ) due to the ballistic transport property in CNTs, low intrinsic capacitance, near ideal subthreshold slope (SS) and its CV/I performance is  $13\times$  higher than

the bulk MOSFET [19-31].

In this paper, we design and simulate four types of Colpitts oscillators based on multiple technologies and compared their performances. These include integer order conventional MOSFET based CO, fractional order MOSFET based CO, CNTFET based integer order CO and CNTFET based fractional order CO, all based on 32 nm technology nodes. A rigorous comparative analysis of the key performance measuring parameters has been done for all the circuits. The LC oscillators used in the COs are characterized by their tank circuits. Herein, both the integer order capacitors and the fractional order based pseudo-capacitors have been used for modelling the tank circuits. In conventional oscillators the oscillation frequency depends upon the RC/LC time constant values, however, in the case of fractional order oscillators it further depends on  $\alpha$ , thus providing a greater control and more design freedom. A rigorous simulation study and comparative analysis of the four designed COs have been done. It has been observed that the CNTFET fractional order CO has shown significant improvement in performance measuring parameters, like power consumption, larger constant phase zone, apart from the advantages of being fractional order. The fractional topology provides precise control over phase and frequency of oscillatory output. To the best of our knowledge, this is the first work where CNTFET based CO, both integer and fractional order, has been designed, simulated and compared.

The paper is divided into VII sections. Section I gives introduction. Section II describes the details about CNTFET. Section III explains the fractional order circuitry. Section IV gives insights on the designing of the fractional order topology. Section V lists the proposed oscillator topologies and there analysis Section VI gives the noise analysis of the CO's. Section VII concludes the paper.

## Carbon Nanotube Field Effect Transistors

CNTs are graphene nano thickness sheets rolled into tubes, considered as the fourth allotropic form of carbon, along with the original three, coal, graphite and diamond. They have unique electrical, mechanical, semiconducting properties and exist in two forms; single wall (SW) and wall in a wall structure, called as multiwall (MW), as shown in Figure 1 [19-21]. Sumio Iijima of Japan discovered multiwall (MW) CNT in 1991, followed by single wall CNT in 1993 along with Donald Bethune (independently) [19]. CNTs show both metallic and semiconducting properties (depending on their chirality or chirality vector), have length in few micrometer and diameter ranging from  $<1$  nm to 50 nm. They are the best thermal conductors (better than diamond), have tensile strength  $10^2 \times$  more than that of steel, can have a current density of  $10^3 \times$  than Cu ( $10^9$  A/cm<sup>2</sup>). CNT based field effect transistor (CNTFET) is an important application of CNTs and the first CNTFET is fabricated by S. J. Trans et. al. [21], as shown in Figure 1. Because of the presence of CNT based channel in a CNTFET, it has a capability to outshine conventional MOSFET in future. The CV/I characteristics of a CNTFET is  $\sim 13 \times$  higher than that of a conventional n-MOSFET [20-25].

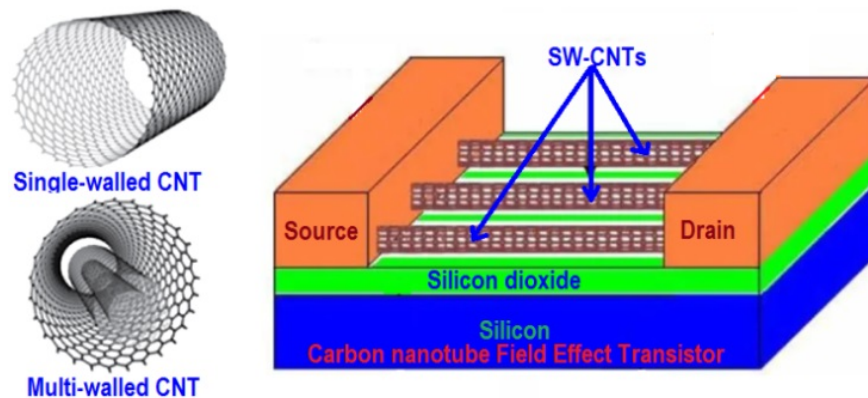


Figure 1: Schematics of SWCNT, MWCNT and a CNTFET

Figure 1 shows the schematics of SW-CNT, MW-CNT and a CNTFET. In this work, 32nm technology node n-type CNTFETs with 1V operating voltage, have been used in the CNTFET based CO circuitry, using HSPICE. Further, Verilog-A Stanford model for CNTFET and BSIMv4.6.1 Berkeley Predictive Technology (BPT) for the conventional MOSFET have been used in the simulation study [20, 21-25]. The various CNT parameters used in the simulations include dielectric constant of 16, CNT-diameter ( $D_{CNT}$ ) of 1.5 nm, inter-CNT pitch (S)-20 nm, threshold voltage ( $V_{TH}$ ) of 0.49 and the chiral vectors (19,0).

## Fractional Calculus Background

The design of analog electronic circuits is based on implementing mathematical operations using the components, like ideal resistor, inductor and capacitor as linear elements. These elements correspond to well-known operations in calculus and therefore are used to realize differential equations of any integer order [9-11]. Real electronic components depart from the ideal behavior and the extent of this departure is expressed in terms of the Q (quality) factor which accounts for these issues. The ideal network components provide a fixed phase shift to all frequencies which pass through them, but all real components show parasitic impedances which cause the phase difference to change with the frequency of the signal passing through them. A fractional impedance or fractance is an impedance whose Laplace transform has a fractional order of the form  $ZF \text{ FRAC}(s, \alpha) = 1 F.s^\alpha$ . Fractional order elements provide a fixed phase shift over a wide range of frequencies and a slope of  $-20\alpha$  dB per decade on Bode plot. By manipulating the order of the fractional element, a component which provides a custom phase shift over a wide frequency range can be created. This new found freedom to control the magnitude and phase of a network independently has already proven useful in modelling systems where cumbersome integer order models are required to reap the benefit provided by simpler fractional order models. Several complex systems also lend themselves to fractional order analysis for better understanding [11-14]. An LC circuit containing a fractional order circuit exhibits a low roll-off of phase response while the magnitude rolls off at a much gentler rate. A fractional order LC circuit can therefore reject out of band noise, leading to lower jitter noise than non-harmonic oscillators. This gives the impression of a much lower Q factor in the phase response than what is apparent in the magnitude response. Fractional calculus (FC) has been there since the time of well-known integral calculus (IC). However, fractional calculus progressed slowly due to the lack of tools, definitions and complexity [1-5]. Fractional Order differential equations were first postulated by Leibniz as a curiosity which might lead to greater insight later [32-34]. Examples of fractional order impedances occur in biological samples whenever a fractal structure exists and power law diffusion occurs. Fractional order capacitors have been artificially made by using super-capacitors, active impedance generators; fractal design patches deposited on silicon and carbon nanotube epoxy devices [9], [17], [11], [18].

### *Realizing Fractional Capacitor for the Proposed Oscillator Designing*

The work on realizing the fractional order capacitors is going on since decades [7-9], however, still they are not available on a commercial scale. Various approximation techniques are being considered to depict the fractional characteristics in a circuit. For a fractional capacitor, the impedance can be represented as:

$$Z(j\omega) = \frac{1}{C(j\omega)^\alpha}$$

$$Z(s = j\omega) = \frac{1}{Cs^\alpha}$$

This expression has a constant phase which equals to  $(-\alpha\pi/2)$  and is dependent upon  $\alpha$ , the fractional order. Therefore a close optimization network is required to be designed that closely mimics this behavior. Fractional order capacitors are approximated by using a geometrically progressive RC ladder structure. These structures are used to implement tank circuits with low phase shift and are used to create fractional order oscillators. The LC circuits built using these capacitors are tested using AC sweeps in order to create Bode plots and verify fractional order reactance [32]. The only drawback is that the huge network comprising of R and C of different values tends to increase the economic cost and space occupied by these ladder circuits.

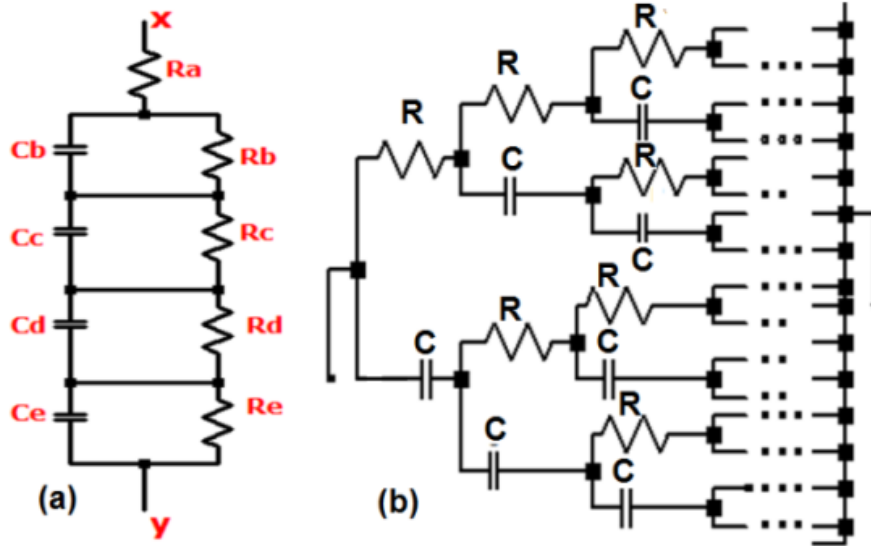


Figure 2 : (a) Single stage RC tree. (b) Equivalent RC tree for fractional order capacitor of any order [8, 16].

Figure 2(a) represents a single stage RC ladder structure for designing a pseudo-capacitance of a particular fractional order( $\alpha$ ) and figure 2(b) shows an equivalent RC tree formed by cascading many such individual single stage RC networks as in figure 2(a) for better approximations of frequency and phase over a particular frequency range.

### RC Ladder component values generation.

Fractional order capacitors are generated for various orders; both fractance and their frequency response curves are studied herewith. This is done to ensure whether the designed pseudo-capacitances have fractional behavior or not in a desired frequency and phase spectrum. Figure 3 depicts a RC ladder of  $n$  equivalent stages. The values of resistors and capacitors of the progressive ladder structure vary based on the fractional order,  $\alpha$ , for which the fractance has been designed (keeping the pseudo-capacitance value same). Keeping the fractance value same, magnitude curves have been plotted for different fractional orders,  $\alpha$  ranging from 0.2 to 0.9, as can be seen in Figure 4. The simulated R and C values for the ladder network have also been taken for various fractional orders ranging from,  $\alpha=0.2$  to  $\alpha=0.9$ . Table 1 depicts the ladder values for same fractance,  $F=10n$ , at different order,  $\alpha$  varying from 0.2 to 0.9. Although, the pseudo-capacitance is same, that is  $F=10n$ , the design using different fractional order  $\alpha$  offers different properties to the fractance device. FOCs offer a unique phase and frequency control by changing  $\alpha$ , keeping the magnitude fixed.

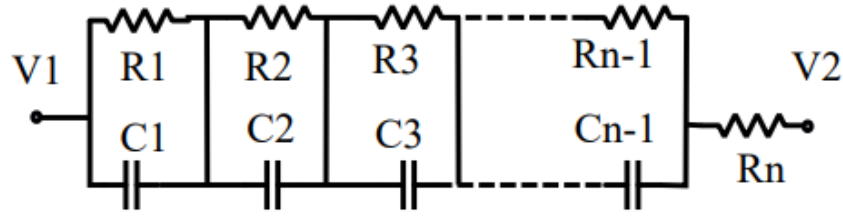


Figure 3: RC Ladder component values generation.

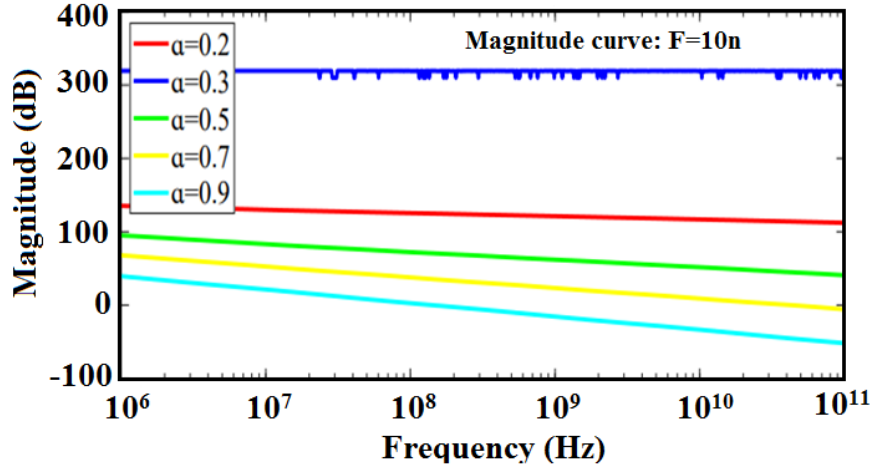


Figure 4: Magnitude response of approximated fractional capacitor with different orders.

The phase response for the designed FOC of value  $F=10n$  has been shown in Figure 5. It shows that with the change in order ' $\alpha$ ', the phase response curve changes even though the magnitude of the designed fractance remains the same. Large ripple value has been obtained for the fractional order  $\alpha=0.3$  over the entire frequency spectrum. The R and C values generated for order,  $\alpha=0.3$  doesn't generate a constant phase zone over the designed range for magnitude  $10n$ , as depicted in Figure 5. As can be seen a lot of ripples are obtained in the frequency spectrum ranging from  $100MHz$  to  $100GHz$ . This is the reason that the simulated FOC of order  $\alpha=0.3$  has not been used in the design and analysis of CO in this work.

Table I: Fractional order RC ladder component values with same Fractance  $F=10n$

| a       | 0.2        | 0.2      | 0.3       | 0.3      | 0.5      | 0.5      | 0.7     | 0.7      | 0.9      | 0.9      |
|---------|------------|----------|-----------|----------|----------|----------|---------|----------|----------|----------|
| Element | R          | C        | R         | C        | R        | C        | R       | C        | R        | C        |
| 1       | 1648791.84 | 5.07E-14 | 490150.24 | 2.13E-13 | 38099.04 | 4.40E-12 | 3054.87 | 9.47E-11 | 272.32   | 2.14E-09 |
| 2       | 1294593.47 | 6.46E-14 | 364255.29 | 2.86E-13 | 24449.62 | 6.86E-12 | 1536.94 | 1.88E-10 | 75.76    | 7.68E-09 |
| 3       | 937097     | 1.77E-14 | 219432.22 | 8.77E-14 | 9503.63  | 2.67E-12 | 320.24  | 9.61E-11 | 4.13     | 5.56E-09 |
| 4       | 678321.66  | 4.87E-15 | 132188.89 | 2.69E-14 | 3694.09  | 1.04E-12 | 66.72   | 4.91E-11 | 0.23     | 4.02E-09 |
| 5       | 491006.02  | 1.34E-15 | 79632.34  | 8.24E-15 | 1435.9   | 4.03E-13 | 13.9    | 2.51E-11 | 0.01     | 2.91E-09 |
| 6       | 355416.8   | 3.67E-16 | 47971.58  | 2.53E-15 | 558.14   | 1.57E-13 | 2.9     | 1.28E-11 | 0        | 2.11E-09 |
| 7       | 257269.97  | 1.01E-16 | 28898.72  | 7.74E-16 | 216.95   | 6.09E-14 | 0.6     | 6.53E-12 | 1.83E-05 | 3.05E-09 |
| 8       | 186225.96  | 2.77E-17 | 17408.97  | 2.37E-16 | 84.33    | 2.37E-14 | 0.06    | 6.67E-12 | 6.87E-07 |          |
| 9       | 134800.46  | 7.60E-18 | 12465.67  | 1.45E-16 | 16.39    | 1.84E-14 | 0.02    |          |          |          |

|    |          |          |        |       |
|----|----------|----------|--------|-------|
| 10 | 48787.94 | 4.17E-18 | 5243.7 | 13.48 |
| 11 | 2185.17  |          |        |       |

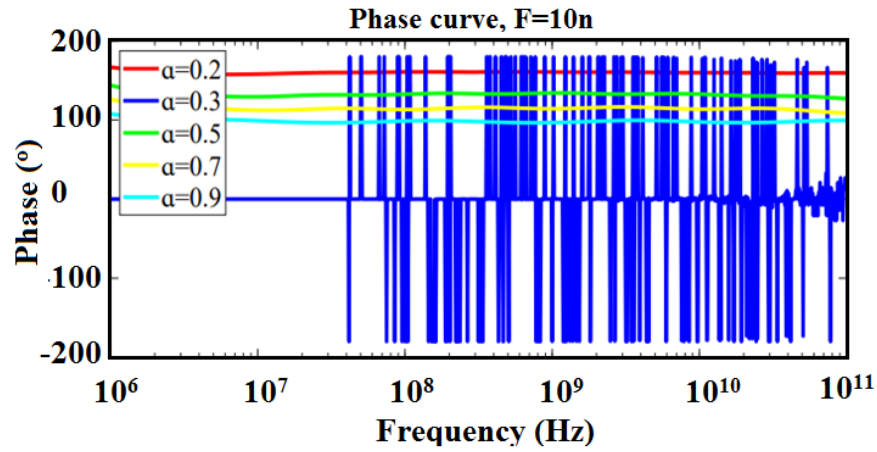


Figure 5: Phase response for different orders.

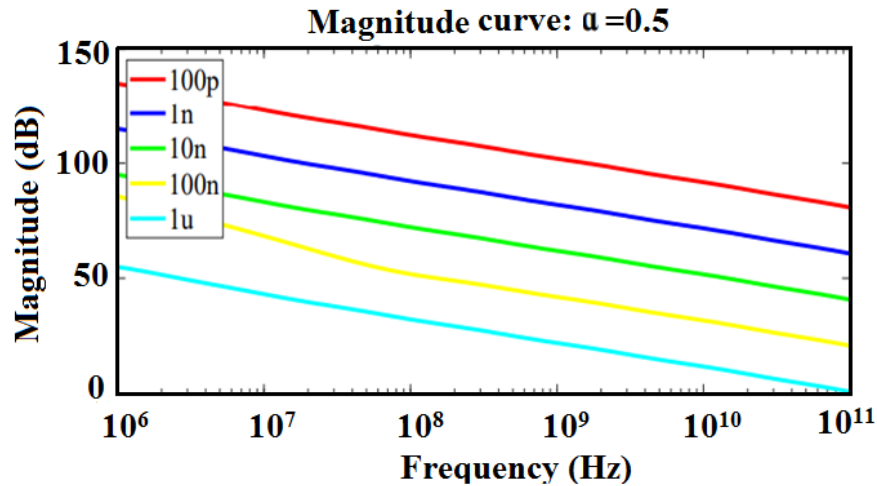


Figure 6: Magnitude curves of various fractance at the same order ( $\alpha=0.5$ )

Figure 6 shows the magnitude response plotted for different fractional capacitors for the same fractional order  $\alpha=0.5$ . It has been observed that larger the magnitude of pseudo-capacitance, greater is the phase (in degrees) obtained. For values less than 100n the phase response values are too low to be plotted, as shown in Figure 7

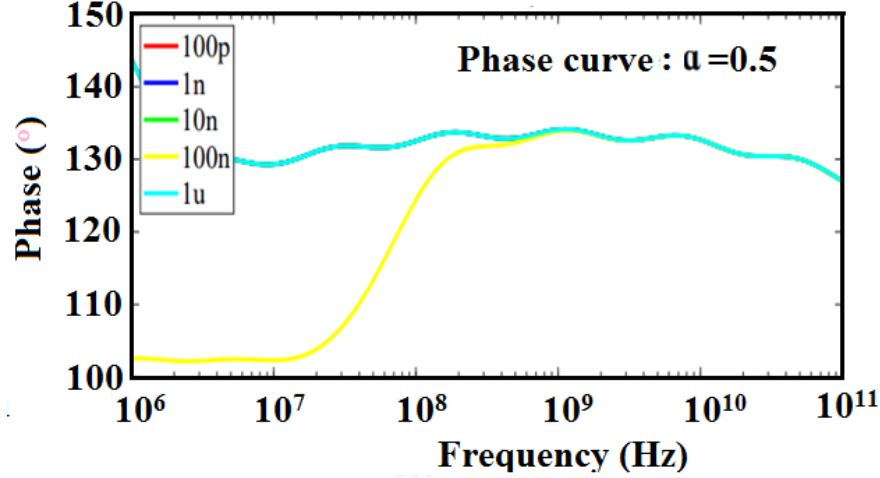


Figure 7: Phase curves for different FOC's at identical  $\alpha$ .

## Proposed Oscillator Topologies

A Colpitts oscillator (CO) is made up of an amplifier and a feedback network, consisting of an inductor and two capacitors. The feedback network is employed to direct a portion of the output signal back to the input through one of the reactive elements. Usage of feedback network provides both the frequency selection and signal reinforcement (positive feedback). For a CO, the oscillation frequency is dependent on its tank circuit elements L and the capacitive divider circuit, as given below.

$$f_{osc} = \frac{1}{2\pi\sqrt{LC_t}} \text{ and } C_t = \frac{C_1 C_2}{C_1 + C_2}$$

The MOS based oscillator can be analyzed by using its tap ratio that is given by:

$$n = 1 + \frac{C_2}{C_1}$$

### Integer order Colpitts Oscillator

Initially, in this work, we design and simulate a conventional MOSFET (32 nm technology node) based single ended CO, as shown in Figure 8. In simulations a 32nm PTM model of MOSFET (L=32 nm and W=180 nm) has been used, along with RL=1k, C1=C2=0.3n and  $I_{bias}=5mA$ . The value of inductor has been varied (keeping other parameters same) to check its effect on the oscillation frequency. The oscillation frequency is 1.2GHz for L=100p and 13.11 GHz for L=1p. Scaling down one of the elements of the tank circuit has a huge impact on its circuit oscillation frequency. On performing the transient analysis with both L=100pH and L=1pH, decaying oscillations can be observed with peak at approximately 0.999 Volts, as shown in Figure 9(a,b).

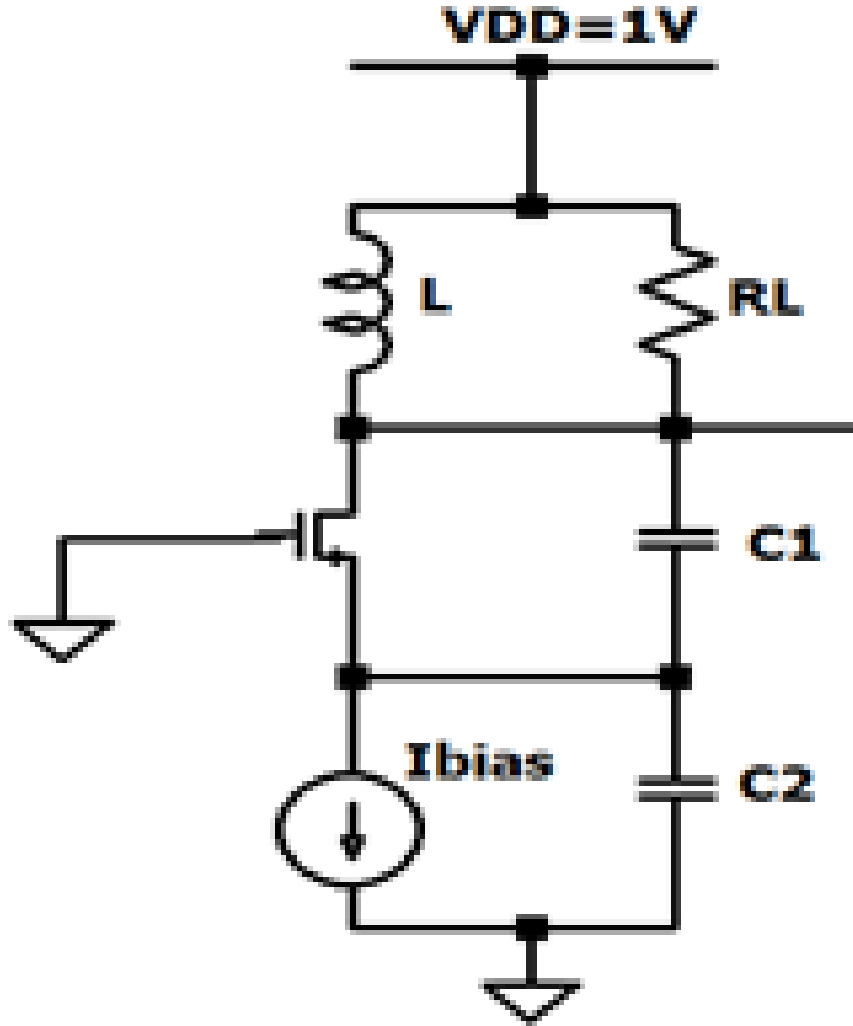


Figure 8: Conventional MOSFET based CO (32nm node)

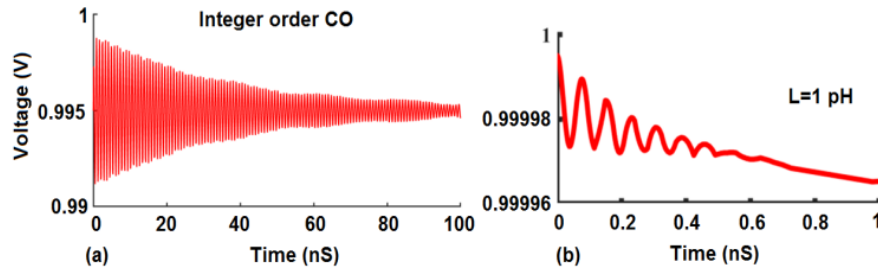


Figure 9: Transient analysis of integer order CO with (a)  $L=100p$  and (b)  $L=1p$ .

After the transient analysis, AC analysis has been performed. The AC analysis involves computing the AC complex node voltages as a function of frequency using an independent voltage or current source as the driving signal. For this a dc voltage source ( $V_{dc}=1V$ ) is employed to provide excitation to the oscillator. This gives the small signal analysis results with variation of magnitude as frequency varies.

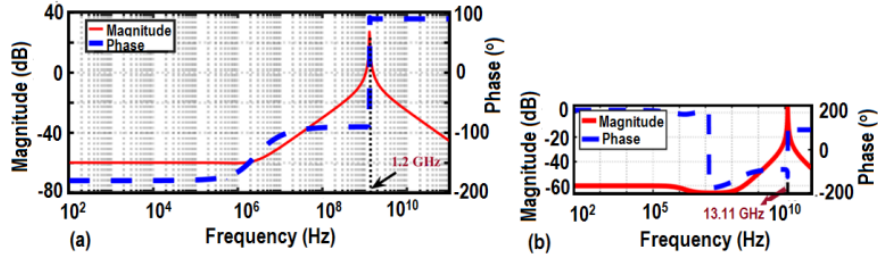


Figure 10: Bode plot for integer order CO with (a)  $L=100\text{pH}$  and (b)  $L=1\text{pH}$ .

Figure 10 shows the Bode plot, showing both the phase and magnitude, for the integer order CO with different  $L$ s,  $L=100\text{pH}$  and  $1\text{pH}$ . At the intersection of magnitude and phase plots, the x-axis gives the frequency of oscillation, as can be seen in Figure 10 (a,b). However, with conventional integer order CO the oscillation frequency for the same set of parameters remains fixed. Both magnitude and phase curves follow a conventional pattern at certain values of circuit parameters. This led to the replacement of integer order theory with robust fractional order theory. Fractional order elements allow efficient control over phase, magnitude and frequency of the designed circuit. Keeping the component values same and varying the fractional order  $\alpha$  generates different results. This allows more design freedom and captures the real analysis paradigm since most of the things have a fractional chaotic behavior.

## Fractional order MOSFET based Colpitts Oscillator

Fractional circuit can be designed by replacing one or more capacitors with fractance devices of known value and a certain fractional order,  $\alpha$ .

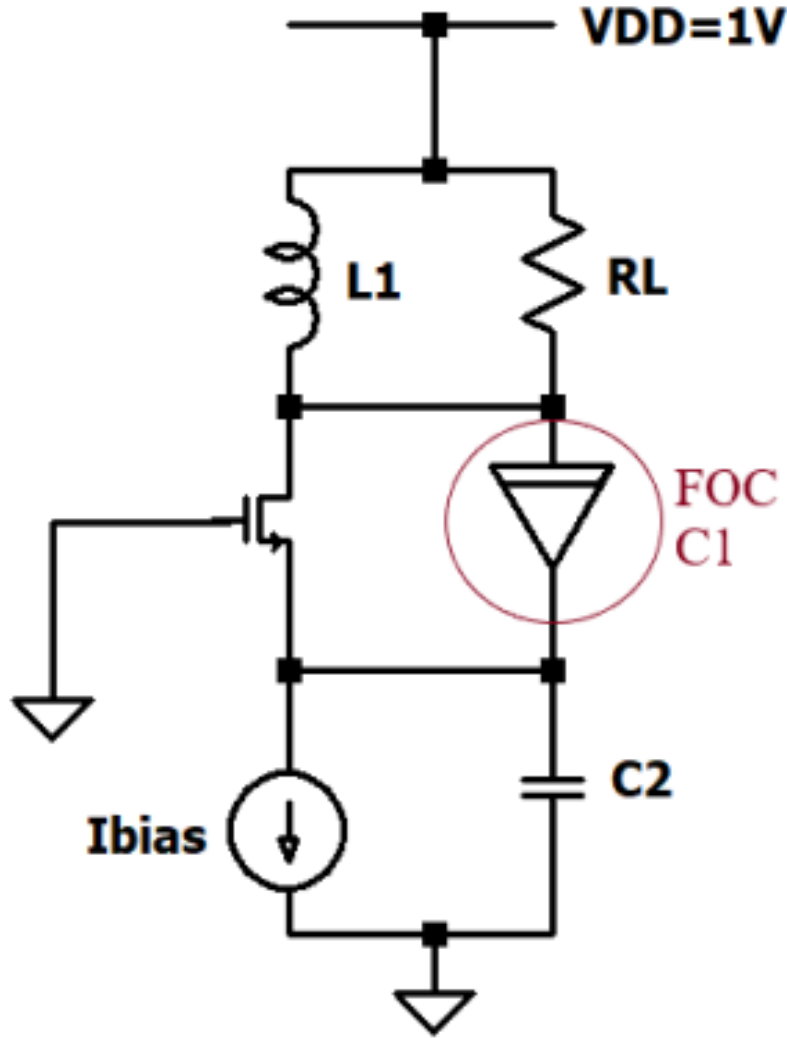


Figure 11: Conventional MOSFET based Fractional order CO.

Figure 12 shows the schematic of the proposed MOSFET based fractional order CO employing one FOC. The tap ratio remains fixed to 2 ( $C1=C2$ ). Herein,  $C1$  of integer value  $0.3n$  has been replaced by a pseudo-capacitance of the same value with different fractional orders,  $\alpha$ . At different fractional orders, the AC response curves of FOC ( $0.3nF s^{1-\alpha}$ ,  $\alpha$ =fractional order) have been obtained. This is done to ensure that the simulated FOCs of value  $0.3nF$  are depicting fractional behavior in a given frequency domain. Progressive RC ladder structures have been used for the designing of fractional capacitors. The component values achieved by simulation via MATLAB for few orders ( $F=0.3n$ ) have been listed in Table II.

Table II: Values of RC ladder components for various orders.

| $\alpha=0.4$ | $\alpha=0.4$ | $\alpha=0.52$ | $\alpha=0.52$ | $\alpha=0.73$ | $\alpha=0.73$ |
|--------------|--------------|---------------|---------------|---------------|---------------|
| R            | C            | R             | C             | R             | C             |
| E5           | E-13         | E5            | E-13          | E4            | E-11          |
| 8.7135       | 0.170        | 3.031         | 0.5811        | 1.2927        | 0.245         |

| $\alpha = 0.4$ | $\alpha = 0.4$ | $\alpha = 0.52$ | $\alpha = 0.52$ | $\alpha = 0.73$ | $\alpha = 0.73$ |
|----------------|----------------|-----------------|-----------------|-----------------|-----------------|
| 5.8358         | 0.253          | 1.912           | 0.9225          | 0.616           | 0.514           |
| 2.5604         | 0.092          | 0.706           | 0.3678          | 0.113           | 0.274           |
| 1.1233         | 0.033          | 0.260           | 0.1466          | 0.0208          | 0.146           |
| 0.4929         | 0.012          | 0.096           | 0.0585          | 0.0038          | 0.078           |
| 0.2162         | 0.0045         | 0.035           | 0.0233          | 0.007           | 0.041           |
| 0.0949         | 0.0017         | 0.013           | 0.0093          | 0.001           | 0.044           |
| 0.0208         | 0.0012         | 0.002           | 0.0074          | 0.000           |                 |
| 0.0222         |                | 0.0018          |                 |                 |                 |

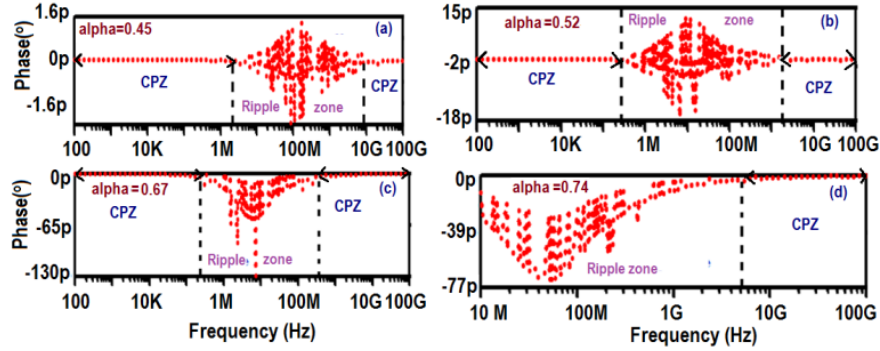


Figure 12: AC responses of pseudo-capacitance 0.3n for different  $\alpha$ .

The designing of FOCs is validated by the presence of their constant phase zones (CPZ). It has been observed that the fractance devices show constant or near constant behavior in terms of phase shift for the entire frequency band [32]. Figure 12 shows the constant phase zones of pseudo-capacitance 0.3n for orders 0.45, 0.52, 0.67 and 0.74. The plots show that other than a small ripple zone, the phase remains constant over most part of the frequency spectrum. The CO with  $C_1=C_2=0.3n$  in the integer domain gave oscillation frequency of 1.2GHz (simulated) with 100pH inductor. However, the same value of pseudo-capacitance, i.e. 0.3n with fractional order 0.4 results in a transient of oscillation frequency 1.7GHz. Further, by varying  $\alpha$  with the same numerical value of capacitance generates plots of different frequency, thereby offering an extra degree of freedom in fractional calculus.

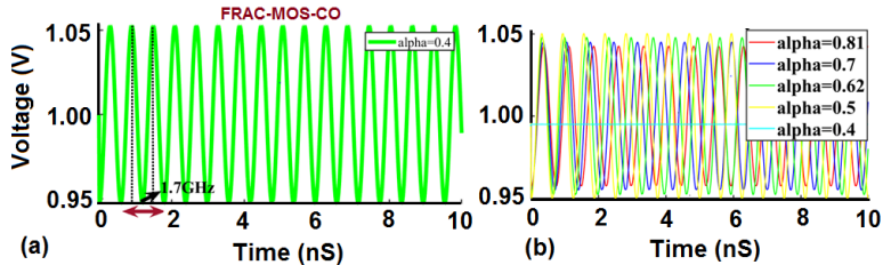


Figure 13: Transient analysis for the fractional order MOS based CO with (a)  $\alpha=0.4$  and (b) for other values of  $\alpha$ .

On varying the fractional order  $\alpha$ , from 0.4 to 0.81, there is a change in the transient characteristics as depicted in Figure 13. Furthermore, the Fast Fourier Transform (FFT) analysis for different fractional orders has

been performed to get the frequency content information, as shown in Figure 14. The FFT converts a signal into its individual spectral components and thus provides the signals frequency information.

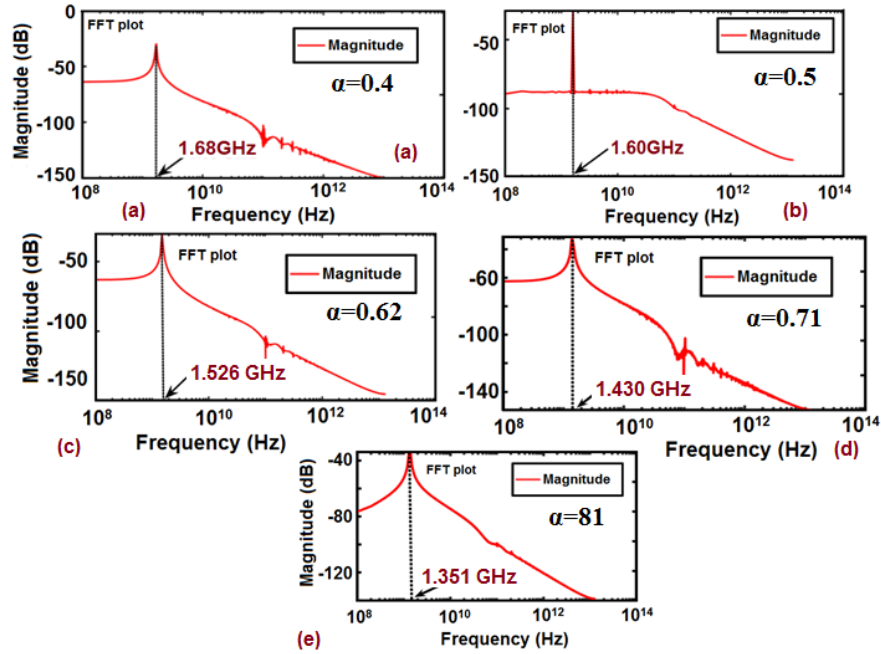


Figure 14: The FFT plots for different fractional orders.

On analyzing the FFT plots, it has been observed that the oscillation frequency tends to decrease slightly on increasing the fractional order, being 1.68 GHz at  $\alpha=0.4$  and 1.351 GHz at  $\alpha=0.81$ . Since the capacitor being fractional of order  $\alpha$  in the CO design, it results in a  $2+\alpha$  circuitry. The designed fractional order CO has an order in the range  $2<\alpha<3$ . If both the capacitors are replaced by FOCs of different orders it enables us to have a greater degree of freedom. The replacement by a higher order FOC increases the system accuracy, thus higher order systems in fractional domain are being considered.

Figure 15: Different orders fractional capacitances.

In Figure 15, the two capacitors have been replaced by FOCs of different order. This results in  $C1=0.3n s^{-0.19}$  and  $C2=C3= 0.3 s^{-0.38}$  :

$$n = 1 + \frac{C_2 + C_3}{C1}$$

$$n = 1 + \frac{0.6}{0.3}$$

$$n = 3$$

A higher tap ratio implies a greater feedback fraction in the oscillator design. For the CO with different order FOCs, an analysis of transient characteristics is performed by varying the inductor values, as shown in Figure 16.

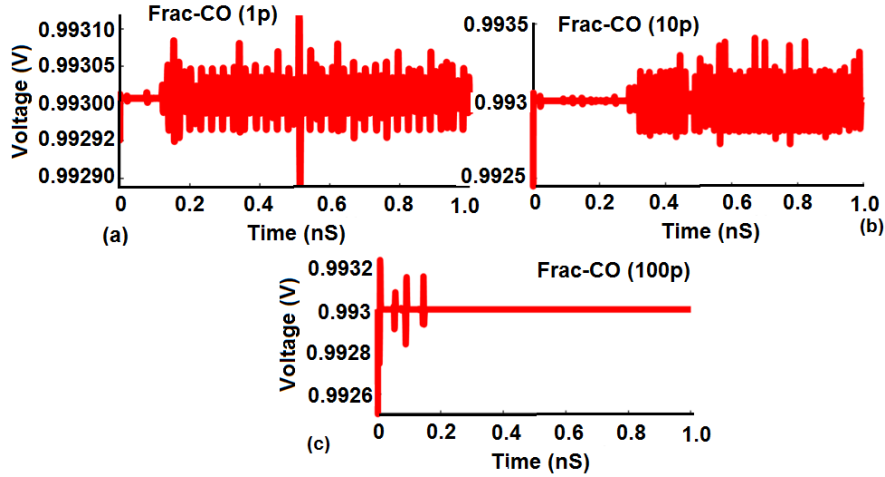


Figure 16: Variation of transient response of fractional order MOS based CO with component resizing (Two fractance devices).

On resizing the value of inductor from 1pH to 100pH, it can be seen from the transient analysis that the frequency tends to decrease for larger value of inductor  $L$ . The peak voltage value also tends to reduce on using two fractance devices of different orders compared to one FOC as in Figure 9. If tap ratio ( $n=2$ ) is used for  $C1=C2=0.3n$  for order,  $\alpha=0.67$  the MOS oscillator oscillates at 1.5GHz as in bode plot representation of Figure 17. This implies that just by varying the order, number of fractance in the circuit, the characteristic properties can be changed.

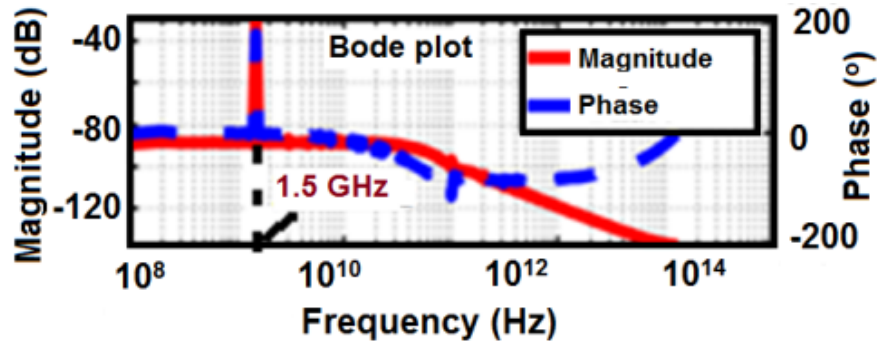


Figure 17: Bode plot for both C1 and C2 fractional with order  $\alpha=0.67$

Fractance devices behave as CPE (Constant Phase Elements). Their phase remains constant over a wide frequency range. They have a wide range of applications for example in electrochemistry, thermal engineering, acoustics, electromagnetism, modeling, time- and frequency-domain system identification and control theory, robotics, and fractal theory [34].

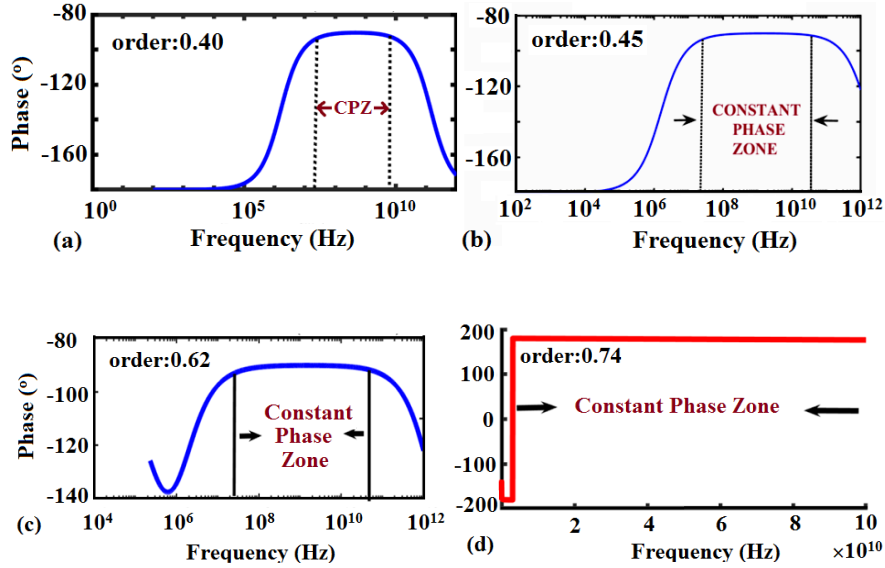


Figure 18: CPZ for (a)  $\alpha=0.4$  (b)  $\alpha=0.45$  (c)  $\alpha=0.62$  and (d)  $\alpha=0.4$

When these FOCs are placed in the oscillator circuitry, constant phase zones are obtained in the phase response analysis too. The constant phase behavior of the conventional MOS based CO, have been obtained for three different orders, as shown in Figure 18. It can be seen that as the order increases there is an increase in the constant phase spectrum. The designed FOCs using passive RC ladder approximation technique generates CPZ in a wide frequency range when placed in a CO circuitry. This is another advantage of fractional order over integer based circuits. Further, the power analysis has been done and it has been observed that there is higher power consumption in fractional order circuitry compared to the normal integer counterparts. For identical circuit parameters, 19.5% increase in power is obtained for fractional order CO circuit (11.82mW,  $\alpha=0.62$ ) compared to the conventional CO (9.997 mW,  $\alpha=0.62$ ). Thus, though desired control and better phase approximations are achieved, however, these ladder circuits being huge cascade connection of resistors and capacitors tend to increase the power consumption as well as the noise in the circuit too. Noise analysis has been done in later in the paper.

## CNTFET based integer order Colpitts Oscillator

To remove the drawbacks of conventional MOSFET based fractional order circuit we move towards a more optimum low power design approach using CNTFETs. The CNTFET based circuits are known to offer lesser static power dissipation due to lower  $I_{OFF}$  and significantly lesser dynamic power due to lower gate capacitance  $C_{GG}$ .

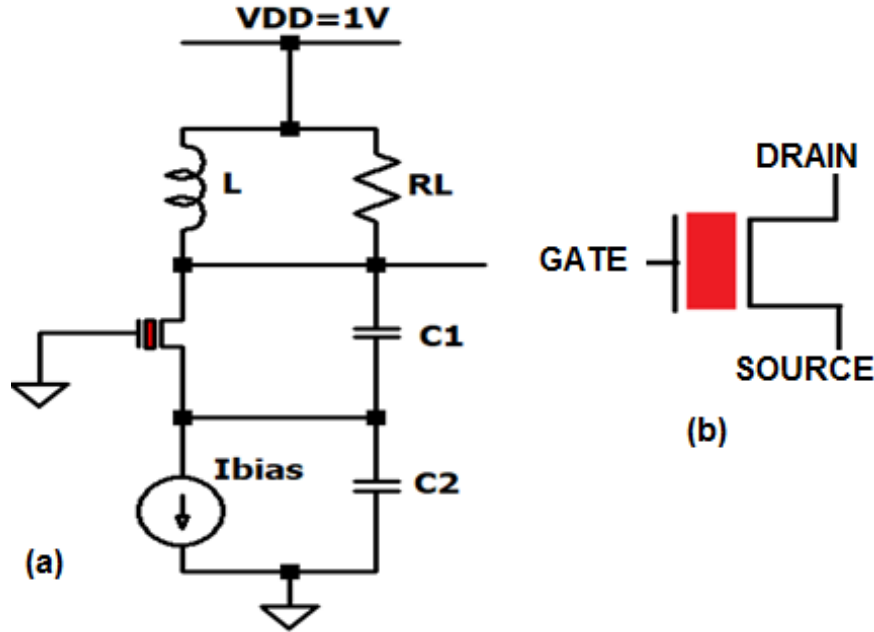


Figure 19. (a) CNTFET based CO (b) symbol used for CNTFET

Figure 19 shows a 32nm CNTFET based integer order CO. Keeping all other parameters same and just varying the inductor values, the oscillation frequency increases from 1.3GHz and 13.11 GHz for  $L=100\text{p}$  and  $L=1\text{p}$  respectively. This can be validated from the bode plots for both the inductor values individually, as shown in Figure 20. Compared to its MOS integer topology, an increase in oscillation frequency is observed in it. The oscillation frequencies achieved for the proposed integer order CNTFET based CO for  $L=100\text{pH}$  and  $L=1\text{pH}$ , with  $C1=C2=0.3\text{n}$  are 1.3GHz and 13.11 GHz respectively.

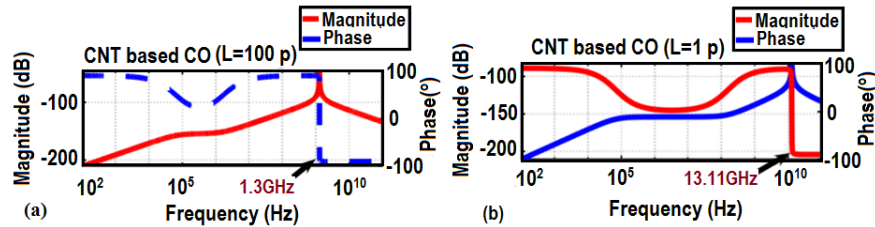


Figure 20: Bode plot of CNTFET based CO for (a)  $L=100\text{pH}$  and (b)  $L=1\text{pH}$ .

The transient analysis for the integer order CNTFET COs have been obtained for both  $L=100\text{pH}$  and  $L=1\text{pH}$  inductor as shown in figure 21 and 22 below:

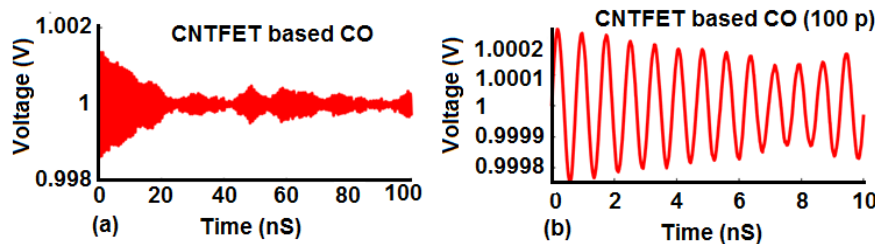


Figure 21: (a) Transient Analysis (b) zoomed for  $L=100p$ .

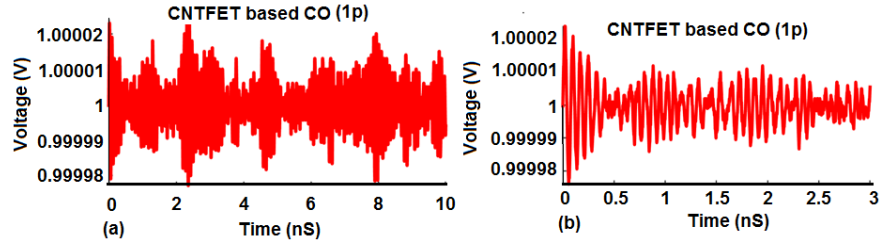


Figure 22: (a) Transient Analysis (b) zoomed for  $L=1pH$

Table III: CNT based CO power compared to MOS based CO and fractional MOS based CO.

$L=100pH$  5mA tail current

| MOS CO                       | FRAC CO ( $\alpha=0.62$ )    | CNT CO                       |
|------------------------------|------------------------------|------------------------------|
| 9.997mW                      | 11.82mW                      | 27.653uW                     |
| $L=100pH$ 500nA tail current | $L=100pH$ 500nA tail current | $L=100pH$ 500nA tail current |
| -                            | -                            | 6uW                          |

A comparative analysis of power consumption has also been performed. It can be seen from Table III that the power dissipated is the least for CNTFET based CO. When tail current is varied from 5mA to 500nA for the case of CNTFET based oscillator, there is a significant reduction in power consumption. Analysis of individual fractional and CNTFET topologies have been performed and compared with conventional MOS topology. It has been observed that a significant decrease power consumption is achieved in the CNTFET based CO in comparison to the conventional MOS based CO. This is attributed to the unique characteristics of CNTs as discussed above.

### CNTFET based fractional order Colpitts Oscillator

To tap the advantages of both CNTFET and fractional order domain, a CNTFET based fractional order CO is designed and analyzed. Figure 23(a) shows the circuit diagram of the proposed fractional order CO, with  $\alpha=0.62$ . Figure 23(b) shows the transient analysis of the proposed CNTFET based fractional order CO.

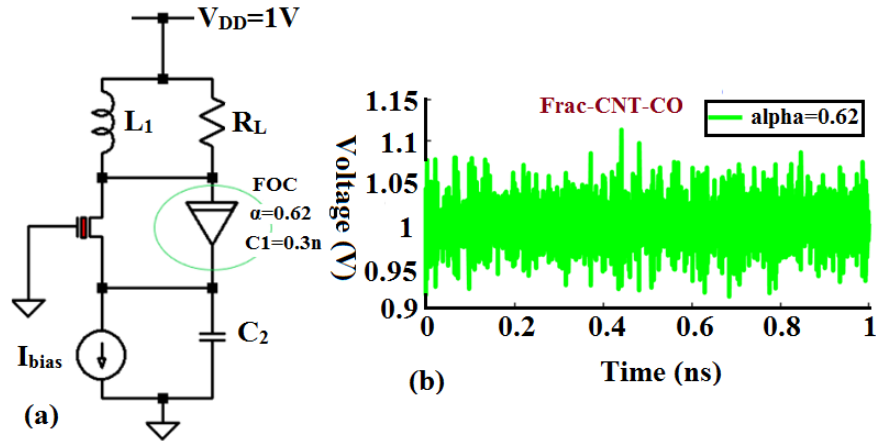


Figure 23: (a) CNTFET based fractional order CO with  $\alpha=0.62$  (b) its transient analysis

Table VI: Effect of variation in average power with change in bias current.

| CNT CO                        | CNT FRAC CO ( $\alpha=0.62$ )  |
|-------------------------------|--------------------------------|
| L=100pH Itail=5mA<br>27.653uW | L=100pH Itail=5mA<br>158.66uW  |
| L=100pH Itail=500nA<br>6uW    | L=100pH Itail=500nA<br>48.75uW |

When a fractional capacitor is used in a CNTFET based fractional order CO, there is a significant increase in power consumption. This is so because FOCs have been realized by using RC ladders. With the change in tail biasing current for both integer order CNTFET based CO and fractional order CNTFET based CO, the average power dissipated reduces as current reduces from 5mA to 500nA, as shown in Table IV. Although there is an increase in power consumed with the insertion of fractional capacitor, however, the FOCs tend to increase the constant phase zone in the phase response curve as depicted in Figure 24.

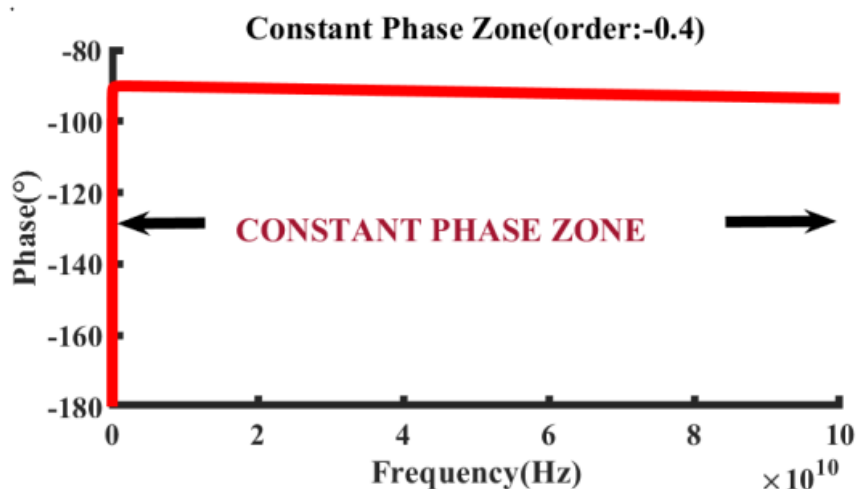


Figure 24: CPZ for the proposed CNTFET-fractional order CO with  $\alpha=0.4$

A comparatively larger CPZ is obtained on integrating fractional circuitry to CNTFET based CO spanning from 100Hz- 100GHz when analyzed using the same order ( $\alpha=0.4$ ) for fractional CO and CNTFET fractional CO as can be seen on comparing figures 24 and 20(a). The FOC of order  $\alpha=0.4$  gives a CPZ of 10MHz-10GHz in the fractional MOS based CO. Integrating CNTFET with FOCs results in a wider constant phase spectrum.

## Noise Analysis of the Designed COs

In this section, the noise analyses of the four COs designed and simulated in this work have been done. Noise is defined as the random fluctuations that affect currents and voltages and it actually sets the lower limit of any signal without its quality being deteriorated. For the conventional MOS based CO, noise analysis takes into account the Thermal noise, Shot noise and Flicker noise. Thermal noise, also called as Nyquist or Johnson noise, is associated with the random thermal motion of charge carriers. Shot noise is caused by

the random fluctuations of the electric current due to electronic charge and the Flicker noise, also called 1/f noise or pink noise, is present in both the active and passive devices and becomes predominant at lower frequencies. In the Stanford CNTFET model no noise source definition exists. However, in various works noise models have been provided as an extension to the Stanford CNTFET model; providing high flexibility to choose the circuit simulators. In this work, an equivalent small signal analysis model and the parameter extraction principle have been employed for the noise analysis of the CNTFET based COs. The intrinsic and extrinsic parameters have been extracted using s-parameter analysis and then subsequently converted to Y and Z parameters. In CNTFETs, the noise modeling can be done in both the saturation and triode regions [26,30]. The various noise sources included in the analysis include thermal noise, shot channel noise and the flicker noise. Figure 25 shows the equivalent circuit of a CNTFET with added noise sources used in analysis. The total noise is the root mean square value of the individual noise contributions.

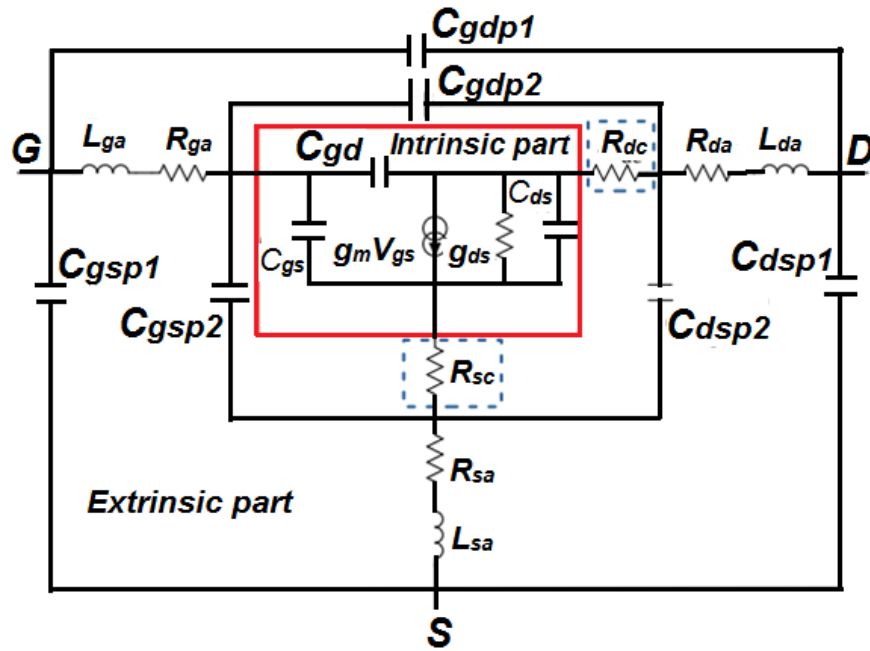


Figure 25: Intrinsic part of the equivalent circuit with added noise sources [26, 3].

To determine noise, the noise spectral density has been computed. Since the power spectral density (PSD) is the square of noise spectral density, therefore, the curves, shown in Figure 26 are an indicative of the power spectrum of output noise too.

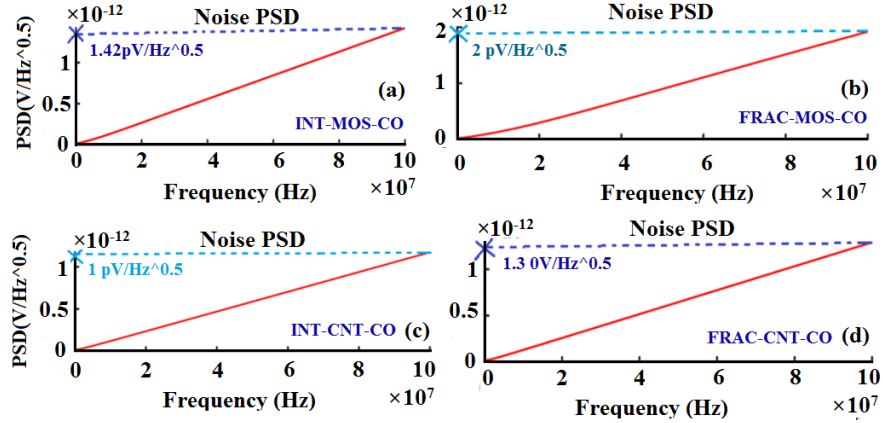


Figure 26: Noise PSD curves for the designed COs (order,  $\alpha=0.62$ ).

From the noise power spectral density curves it can be observed that the peak noise is the least for CNTFET based CO. Fractional MOS based CO is having the highest peak noise value. The peak values of the noise PSD (in  $\text{pV}/\text{Hz}^{0.5}$ ) for different COs are 1.42, 2, 1 and 1.3 for the integer order MOS, fractional order MOS, integer order CNTFET and fractional order CNTFET based COs respectively. The reduced noise in the CNTFET based COs is attributed to significantly reduced resistance in CNTs due to intrinsic ballistic transport in CNTs.

## CONCLUSION

In this work we initially design a Si-MOS based CO in both integer and fractional topologies. Pseudo-capacitances with various fractional orders have been designed and used in the tank circuit of CO. The variation of oscillator properties with fractional order has been discussed in detail. CO made using FOC's consumed comparatively more power and noise. Thus, an optimal design of CO has been made using CNT-FET. The CNTFET based CO consumes much less power compared to both conventional and fractional silicon based oscillators. To tap the advantages of CNTFET and fractional circuitry a CNTFET based fractional order CO is designed and simulated. The CNTFET fractional CO along with low power consumption exerted a greater control over phase and oscillation frequency by changing the fractional order,  $\alpha$ . It has been shown through SPICE and MATLAB simulations that the fractional oscillator based on CNTFET outperforms MOS based fractional oscillator in achieving a wider CPZ for the same fractional order.

## References

1. Behzad Razavi, Design of Analog CMOS Integrated Circuits, McGraw Hill Higher Education, Year: 2003
2. Gray, Analysis and Design of Analog Integrated Circuits, Oxford University Press, USA, Year: 2001
3. Guillermo Gonzalez, Foundations of Oscillator Circuit Design, Artech House, Boston London.
4. Timothy K John, A Colpitts Oscillator Design Technique Using S-Parameters- STARS, University of Central Florida, 1986
5. Experimental demonstration of fractional order oscillators of orders 2.6 and 2.7; Chaos, Solitons and Fractals Nonlinear Science, and Nonequilibrium and Complex Phenomena [Elsevier 2017]
6. D. Mondal, K. Biswas, "Performance study of fractional order integrator using single-component fractional order element," IET Circuits, Devices & Systems, Vol. 5, No. 4, pp. 334-342, July 2011.

7. Z. Gao, X. Liao, “Improved Oustaloup approximation of fractional-order operators using adaptive chaotic particle swarm optimization,” *Journal of Systems Engineering and Electronics*, Vol. 23, No. 1, pp. 145-153, Feb.2012.
8. M. Sivarama Krishna, S. Das, K. Biswas, and B. Goswami, “Fabrication of a fractional order capacitor with desired specifications: a study on process identification and characterization,” *IEEE Transactions on Electron Devices*, vol. 58, no. 11, pp. 4067–4073, 2011.
9. T. Haba, G. Ablart, T. Camps, and F. Olivie, “Influence of the electrical parameters on the input impedance of a fractal structure realised on silicon,” *Chaos, Solitons Fractals*, vol. 24 no. 2, pp. 479–490, 2005.
10. B. T. Krishna and K. V. V. S. Reddy, “Active and passive realization of fractance device of order 1/2,” *Active and Passive Electronic Components*, vol. 2008, Article ID 369421, 5 pages,2008.
11. El-Khazali, Reyad & Tawalbeh, Nabeel. (2012). Realization of Fractional-Order Capacitors and Inductors.
12. Sajad A. Loan, S. Qureshi and S.S.K.Iyer, (2010) A New Partial Ground Plane Based MOSFET on Selective Buried oxide, A 2D simulation study” *IEEE Transactions on Electron Devices*, Vol. 57, No. 3, pp.671-680, 2010
13. F. Bashir, Sajad A. Loan, A.R.M. Alamoud, A High Performance Source Engineered Charge Plasma based Schottky MOSFET on SOI, *IEEE Transactions on Electron Devices*, vol. 9. 2015.
14. I. Podlubny, I. Petra Vs, B. M. Vinagre, P. O’Leary, and L. DorcVak, “Analogue realizations of fractional-order controllers,” *Nonlinear Dynamics*, vol. 29, no. 1–4, pp. 281–296, 2002
15. Ahmad W, El-Khazali R, Elwakil A. Fractional-order wien-bridge oscillator.*Electron Lett* 2001;37(18):1110–12.
16. Radwan A, Soliman A, Elwakil A. Design equations for fractional-order sinusoidal oscillators: four practical circuit examples. *Int J Circuit Theory Appl*2008;36(4):473–92.
17. Zaid Mohammad Shah, Mujtaba Yousuf Kathjoo, Farooq Ahmad Khanday, Karabi Biswas, Costas Psychalinos, A survey of single and multi-component Fractional-Order Elements (FOEs) and their applications, *Microelectronics Journal*, Volume 84, pp.9-25,2019,
18. Si Gangquan, Diao Lijie, Zhu Jianwei, Lei Yuhang, Zhang Yanbin. Attempt to generalize fractional-order electric elements to complex-order ones. *Chinese Physics B*, 2017, 26(6): 060503 .
19. Iijima, Sumio. ”Helical microtubules of graphitic carbon.” *nature* vol. 354, no. 6348 ,pp.56-58, Nov. 1991.
20. Stanford University. (2008). CNFET Model Website, [Online]. Available: <http://nano.stanford.edu./model.php>.
21. S. J. Tans, A. R. Verschueren, and C. Dekker, \Room-temperature transistor based on a single carbon nanotube,” *Nature*, vol. 393, no. 6680, pp. 49{52, 1998.
22. Marani R., Perri A.G.; (2011) A Compact, Semi-empirical Model of Carbon Nanotube Field Effect-Transistors oriented to Simulation Software, *Current Nanoscience*, vol. 7, n. 2, pp. 245-253.
23. Deng J and H S P Wong,” A compact SPICE model for carbon nanotube field effect transistors including nonidealities and its application—Part II: full device model and circuit performance benchmarking ,” *IEEE Trans. Electron Devices* , Vol. 54 , no. 12, pp. 3195–3205,Nov.2007.
24. Jogad S. Sajad A. Loan, Neelofer Afzal, and Abdullah G. Alharbi. ”CNTFET based class AB current conveyor II: Design, analysis and waveform generator applications.” *International Journal of Numerical Modelling: Electronic Networks, Devices and Fields* Vol.34, no. 1 ,e2783, 2021.
25. M.Nizamuddin Sajad A. Loan, Shuja A Abbasi and A. R. M. Alamoud, “Design and Comparative Analysis of High performance cascode carbon Nanotube based operational transconductance amplifiers” *IOP Nanotechnology*, vol. 9, 2015 (SCI Listed; IF=3.82).
26. Javey, Ali & Tu, Ryan & Farmer, Damon & Guo, Jing & Gordon, Roy & Dai, Hongjie. (2005). High Performance N-Type Carbon Nanotube Field Effect Transistors with Chemically Doped Contacts. *Nano letters*. 5. 345-8. 10.1021/nl047931j.
27. J. Deng, H.-S. P. Wong, A Compact SPICE Model for Carbon-Nanotube Field-Effect Transistors Including Nonidealities and Its Application - Part I:Model of the Intrinsic Channel Region, *IEEE*

- Trans. Electron Devices, vol 54, pp. 3186-3194, 2007.
28. J. Guo, S. Hasan, A. Javey, G. Bosman, and M. Lundstrom, "Assessment of high-frequency performance potential of carbon nanotube transistors," *IEEE Transactions on Nanotechnology*, vol. 4, pp. 715-721, 2005.
  29. Ramos-Silva, J. N., Pacheco-Sánchez, A., Enciso-Aguilar, M. A., Jiménez, D., & Ramírez-García, E. (2020). Small-signal parameters extraction and noise analysis of CNTFETs. *Semiconductor Science and Technology*. <https://doi.org/10.1088/1361-6641/ab760b>
  30. M. Hartmann et al., "CNTFET Technology for RF Applications: Review and Future Perspective," in *IEEE Journal of Microwaves*, vol. 1, no. 1, pp. 275-287, Jan. 2021, doi: 10.1109/JMW.2020.3033781
  31. Fei Liua\_ and Kang L. Wang ,Daihua Zhang and Chongwu Zhou "Noise in carbon nanotube field effect transistor", *APPLIED PHYSICS LETTERS* 89, 063116 \_2006\_ <https://www.microwaves101.com/encyclopediass / parameter>
  32. M. Sugi, Y. Hirano, Y. F. Miura, and K. Saito, "Frequency behavior of self-similar ladder circuits," *Colloids and Surfaces A: Physicochemical and Engineering Aspects*, vol. 198-200, pp. 683-688, Feb. 2002
  33. Ondrej Domansky·,Roman Sotner,Lukas Langhammer "Practical Design of RC Approximants of Constant Phase Elements and Their Implementation in Fractional-Order PID Regulators Using CMOS Voltage Differencing Current Conveyors",Springer Science+Business Media, LLC, part of Springer Nature 2018.
  34. Karabi Biswas, Siddhartha Sen, and Pranab Kumar Dutta "Realization of a Constant Phase Element and Its Performance Study in a Differentiator Circuit".
  35. Jogad, S., Akhoun, M.S. & Loan, S.A. CNTFET based comparators: design, simulation and comparative analysis. *Analog Integr Circ Sig Process* (2023). <https://doi.org/10.1007/s10470-022-02119-7>
  36. S. Mujumdar, S. A. Loan and N. Afzal, "CNTFET based 2-bit Unary weighted Current Steering Digital to Analog Converter using Cascode Current Mirror Technique," 2022 International Conference on Microelectronics (ICM), Casablanca, Morocco, 2022, pp. 70-73, doi: 10.1109/ICM56065.2022.10005533